



U.S. Department  
of Transportation  
Federal Highway  
Administration

PB96101050



Publication No. FHWA-RD-94-174  
OCTOBER 1995

---

# Degradation of Powder Epoxy Coated Panels Immersed in a Saturated Calcium Hydroxide Solution Containing Sodium Chloride

---

Research and Development  
Turner-Fairbank Highway Research Center  
6300 Georgetown Pike  
McLean, Virginia 22101-2296

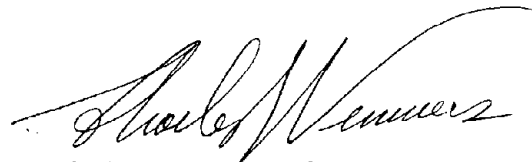
REPRODUCED BY: **NTIS**  
U.S. Department of Commerce  
National Technical Information Service  
Springfield, Virginia 22161

## FOREWORD

This report describes a corrosion study aimed at gaining a better understanding of the material and environmental factors affecting the service life of epoxy-coated reinforcing bars exposed in a simulated marine environment. Corrosion experiments were conducted on approximately 200 steel-coated panels immersed in a calcium hydroxide-saturated solution containing 3.5 percent sodium chloride. The panels were coated with two commercial epoxy powder coatings, at two coating thicknesses (130 and 190  $\mu\text{m}$ ), scribed and unscribed, and immersed in solution at two temperatures (35 and 50  $^{\circ}\text{C}$ ). Panel deterioration was monitored as a function of anodic growth, cathodic delamination, and wet-adhesion loss.

This study concluded that only the scribed panels deteriorated. The scribed panels began to corrode within 24 h after immersion. For panels immersed in the 50  $^{\circ}\text{C}$  solution, the number of anodic sites on a panel did not change after approximately 100 h of immersion. Thus, increases in total anodic area were attributed to the increased growth of existing, individual anodic sites. After 500 h of immersion, electro-osmotic blisters formed above each anode. The hydrostatic pressures within 20 of these blisters were measured in compression. The average compressive stress was 0.84 MPa, with a standard deviation of 0.42 MPa. Several of the electro-osmotic blisters were lanced with a hypodermic needle to extract the blister fluid. The pH of the blister fluid ranged from 5 to 5.5. The concentration of  $\text{Na}^+$  was about the same as in the immersion solution; the  $\text{Cl}^-$  concentration was three to six times greater than the concentration of  $\text{Cl}^-$  in the immersion solution. The anodic corrosion products were mostly a black pasty material that was presumed to be  $\text{Fe}_3\text{O}_4$ .

This report will be of interest to materials and bridge engineers, reinforced-concrete corrosion specialists, organic coating manufacturers, and manufacturers of epoxy-coated reinforcing bars.



Charles J. Nemmers, P.E.  
Director, Office of Engineering and  
Highway Operations Research and  
Development

## NOTICE

This document is disseminated under the sponsorship of the Department of Transportation in the interest of information exchange. The United States Government assumes no liability for its contents or use thereof. This report does not constitute a standard, specification, or regulation.

The United States Government does not endorse products or manufacturers. Trade and manufacturers' names appear in this report only because they are considered essential to the object of the document.

1. Report No. FHWA-RD-94-174		2. Government Accession No.		3. Recipient's Catalog No.	
4. Title and Subtitle DEGRADATION OF POWDER EPOXY-COATED PANELS IMMERSSED IN A SATURATED CALCIUM HYDROXIDE SOLUTION CONTAINING SODIUM CHLORIDE				5. Report Date October 1995	
				6. Performing Organization Code	
7. Author(s) J.W. Martin; T. Nguyen; D. Alsheh; J.A. Lechner; E. Embree; E. Byrd; and J. Seiler				8. Performing Organization Report No.	
9. Performing Organization Name and Address National Institute of Standards and Technology (NIST) Division 862, Building Materials Gaithersburg, MD 20899				10. Work Unit No. (TRAIS) 3D4d	
				11. Contract or Grant No. DTFH61-92-Y-30115	
12. Sponsoring Agency Name and Address Office of Engineering and Highway Operations R&D Federal Highway Administration 6300 Georgetown Pike McLean, VA 22101-2296				13. Type of Report and Period Covered Final Report August 1992 - July 1994	
				14. Sponsoring Agency Code	
15. Supplementary Notes Contracting Officer's Technical Representative (COTR) - Y.P. Virmani, HNR-10					
16. Abstract <p>Blasted-steel panels were coated with two commercial powder epoxy coatings. Approximately half (80) of the coated panels were scribed; while the other half remained defect-free. All of the panels were immersed in a saturated calcium hydroxide solution containing 3.5 percent sodium chloride maintained at either 35 or 50 °C.</p> <p>None of the unscribed panels degraded after 3074 h of immersion at 35 °C; whereas, all of the scribed panels degraded within 24 h after immersion, regardless of the immersion solution temperature. Scribed panels degraded in three ways: (1) anodic corrosion, (2) cathodic disbondment, and (3) wet-adhesion loss.</p> <p>Anodic corrosion was attributed to localized crevice corrosion. The rate of anodic growth depended on the immersion solution temperature, but it did not depend on the type of coating or coating thickness. Liquid-filled blisters formed above the anodic sites after approximately 1000 h of immersion at 35 °C. The chloride concentration of the blister fluid was four times greater than that of the bulk solution and its pH was around 5.</p> <p>The rate of cathodic disbondment was not affected by the type of coating or coating thickness, but it was greatly affected by an increase in the temperature of the immersion solution. Wet-adhesion loss was not affected by coating thickness, but it does depend on the type of coating and immersion temperature. Also, even though the wet-adhesion strength of the two coatings differed by a factor of five, the rate of corrosion for the two coatings was not significantly different.</p>					
17. Key Words Anodic blisters, cathodic disbondment, crevice corrosion, epoxy-coated rebars, infrared thermography, peel, wet adhesion			18. Distribution Statement No restrictions. This document is available to the public through the National Technical Information Service, Springfield, VA 22161		
19. Security Classif. (of this report) Unclassified		20. Security Classif. (of this page) Unclassified		21. No. of Pages 44	22. Price

# SI\* (MODERN METRIC) CONVERSION FACTORS

## APPROXIMATE CONVERSIONS TO SI UNITS

## APPROXIMATE CONVERSIONS FROM SI UNITS

Symbol	When You Know	Multiply By	To Find	Symbol	Symbol	When You Know	Multiply By	To Find	Symbol
<b>LENGTH</b>					<b>LENGTH</b>				
in	inches	25.4	millimeters	mm	mm	millimeters	0.039	inches	in
ft	feet	0.305	meters	m	m	meters	3.28	feet	ft
yd	yards	0.914	meters	m	m	meters	1.09	yards	yd
mi	miles	1.61	kilometers	km	km	kilometers	0.621	miles	mi
<b>AREA</b>					<b>AREA</b>				
in <sup>2</sup>	square inches	645.2	square millimeters	mm <sup>2</sup>	mm <sup>2</sup>	square millimeters	0.0016	square inches	in <sup>2</sup>
ft <sup>2</sup>	square feet	0.093	square meters	m <sup>2</sup>	m <sup>2</sup>	square meters	10.764	square feet	ft <sup>2</sup>
yd <sup>2</sup>	square yards	0.836	square meters	m <sup>2</sup>	m <sup>2</sup>	square meters	1.195	square yards	yd <sup>2</sup>
ac	acres	0.405	hectares	ha	ha	hectares	2.47	acres	ac
mi <sup>2</sup>	square miles	2.59	square kilometers	km <sup>2</sup>	km <sup>2</sup>	square kilometers	0.386	square miles	mi <sup>2</sup>
<b>VOLUME</b>					<b>VOLUME</b>				
fl oz	fluid ounces	29.57	milliliters	mL	mL	milliliters	0.034	fluid ounces	fl oz
gal	gallons	3.785	liters	L	L	liters	0.264	gallons	gal
ft <sup>3</sup>	cubic feet	0.028	cubic meters	m <sup>3</sup>	m <sup>3</sup>	cubic meters	35.71	cubic feet	ft <sup>3</sup>
yd <sup>3</sup>	cubic yards	0.765	cubic meters	m <sup>3</sup>	m <sup>3</sup>	cubic meters	1.307	cubic yards	yd <sup>3</sup>
NOTE: Volumes greater than 1000 l shall be shown in m <sup>3</sup> .									
<b>MASS</b>					<b>MASS</b>				
oz	ounces	28.35	grams	g	g	grams	0.035	ounces	oz
lb	pounds	0.454	kilograms	kg	kg	kilograms	2.202	pounds	lb
T	short tons (2000 lb)	0.907	megagrams (or "metric ton")	Mg (or "t")	Mg (or "t")	megagrams (or "metric ton")	1.103	short tons (2000 lb)	T
<b>TEMPERATURE (exact)</b>					<b>TEMPERATURE (exact)</b>				
°F	Fahrenheit temperature	5(F-32)/9 or (F-32)/1.8	Celsius temperature	°C	°C	Celsius temperature	1.8C + 32	Fahrenheit temperature	°F
<b>ILLUMINATION</b>					<b>ILLUMINATION</b>				
fc	foot-candles	10.76	lux	lx	lx	lux	0.0929	foot-candles	fc
fl	foot-Lamberts	3.426	candela/m <sup>2</sup>	cd/m <sup>2</sup>	cd/m <sup>2</sup>	candela/m <sup>2</sup>	0.2919	foot-Lamberts	fl
<b>FORCE and PRESSURE or STRESS</b>					<b>FORCE and PRESSURE or STRESS</b>				
lbf	poundforce	4.45	newtons	N	N	newtons	0.225	poundforce	lbf
lbf/in <sup>2</sup>	poundforce per square inch	6.89	kilopascals	kPa	kPa	kilopascals	0.145	poundforce per square inch	lbf/in <sup>2</sup>

\* SI is the symbol for the International System of Units. Appropriate rounding should be made to comply with Section 4 of ASTM E380.

## TABLE OF CONTENTS

	<u>Page</u>
CHAPTER 1. INTRODUCTION .....	1
CHAPTER 2. EXPERIMENTAL PLAN.....	3
GENERAL.....	3
MATERIALS .....	3
Substrate.....	3
Coated Panels .....	3
EXPOSURE ENVIRONMENT .....	6
Immersion Solution.....	6
Exposure.....	6
FREE FILMS.....	9
QUANTIFICATION OF DEGRADATION .....	9
Anodic Corrosion .....	10
Elemental Analysis Through a Cross-Section of the Scribe .....	11
Height and Compressive Strength of Anodic Blisters .....	11
Ion Concentrations and pH of Anodic Blister Fluid .....	12
Cathodic Disbondment and Wet-Adhesion Loss .....	12
CHAPTER 3. RESULTS .....	13
FREE FILMS.....	13
UNSCRIBED PANELS .....	13
SCRIBED PANELS .....	15
Anodic Corrosion .....	15
Cathodic Disbondment.....	20
Wet-Adhesion Loss .....	22
CHAPTER 4. DISCUSSION.....	25
UNSCRIBED PANELS .....	25
SCRIBED PANELS .....	25
Anodic Corrosion .....	25
Cathodic Disbondment.....	27
Wet-Adhesion Loss .....	27
CHAPTER 5. CONCLUSIONS .....	29
APPENDIX A. POWER LAW GROWTH OF ANODIC AREA.....	31
REFERENCES .....	35

## LIST OF FIGURES

<u>Figure No.</u>		<u>Page</u>
1.	Location of thickness measurements for all panels being tested.....	5
2.	Schematic of experimental apparatus used in anodic growth studies.....	7
3.	Peel test apparatus for measuring: (1) wet adhesion and (2) the progress of cathodic disbondment.....	8
4.	Thermographic image of the anode next to the scribe mark: (a) thermographic image and (b) computer-enhanced image.....	10
5.	Anodic blister compression measurement.....	11
6.	Location and shape of anodic sites next to scribe mark.....	16
7.	(a) Typical fits of the power law model to 35 and 50 °C total anodic area data as a function of immersion time, (b) straight line fit to panels in which anodic areas were present before the first inspection time, and (c) effect on the fit of the power law model when a panel was removed from the immersion experiment after 500 h.....	17
8.	Plot of power law slope (b) and intercept (a) coefficients for 35 and 50 °C data.....	18
9.	Elemental distribution maps through a cross-section near the scribe mark of a powder epoxy-coated steel panel.....	20
10.	Peel strength as a function of distance from the scribe mark for coated panels immersed for different periods of time.....	21
11.	Maximum disbonded distance from the scribe mark as a function of immersion time.....	22
12.	Wet-adhesion strength loss versus immersion time.....	23
13.	Wet-adhesion strength recovery as a function of drying time.....	24

## LIST OF TABLES

<u>Table No.</u>		<u>Page</u>
1.	Number of panels and the average and standard deviation of the thicknesses of the Coating 1 and Coating 2 panels assigned to the anodic growth experiment.....	4
2.	Physical properties of Coatings 1 and 2 free films.....	14
3.	Coefficients of the power law model.....	31





## CHAPTER 1. INTRODUCTION

A typical concrete bridge deck located in the "snow belt" of the United States in the 1970's required maintenance after 5 years.<sup>(1)</sup> The rapid deterioration of the bridge decks was attributed to the increased use of deicing salts on U.S. roads.<sup>(2,3)</sup> The inherent benefits of using deicing salts were so great, however, that it was not feasible to reduce the applied volume, even though the cost of maintaining bridge decks was becoming prohibitively expensive. Instead, the Federal Highway Administration (FHWA) sponsored a project at the National Bureau of Standards [now called the National Institute of Standards and Technology (NIST)] to identify candidate organic coatings capable of protecting reinforcing steel bars from corrosion. Epoxy powder coatings emerged as the most promising of the coatings studied.<sup>(4)</sup> The first structure utilizing epoxy powder-coated reinforcing steel bars (hereinafter called epoxy rebars) was an experimental bridge built in 1973 in West Conshohocken, Pennsylvania.<sup>(2)</sup> Since that time, over 100,000 structures containing epoxy rebars have been constructed in the United States.<sup>(5,6)</sup>

In general, the corrosion performance of structures containing epoxy rebars has been praiseworthy.<sup>(7,8)</sup> In the late 1980's, however, the premature deterioration of a number of substructural members was reported in three bridges located in Key West, Florida.<sup>(9-11)</sup> These findings led to claims that: (1) epoxy rebars exposed to marine environments are more susceptible to corrosion than bare steel rebars; (2) epoxy coatings are not effective in providing long-term corrosion protection to reinforcing bars in salt-contaminated concrete; and (3) the technology of organic-coated reinforcing bars, as practiced in North America, is flawed.<sup>(12,13)</sup>

Due to the above, FHWA initiated a research study at NIST to reexamine the effectiveness of epoxy coatings in substructural bridge members exposed in a simulated marine environment.



## CHAPTER 2. EXPERIMENTAL PLAN

### GENERAL

Variables included in this study were two commercial epoxy powder coatings, two coating thicknesses (thick and thin), two coating conditions (unscribed and scribed), and two panel temperatures (high and low).

Two sets of experiments were conducted in parallel. The panels for both experiments were prepared in the same manner, at the same time, and were immersed in the same electrolyte. The first experiment studied anodic growth as a function of immersion time; the second experiment studied cathodic disbondment plus wet-adhesion loss in parallel (hereinafter called the disbondment experiment). The anodic growth measurements were made using a non-destructive technique—*infrared thermography*; whereas, the disbondment measurements were destructive, using a technique specifically developed for this experiment.

### MATERIALS

#### Substrate

A total of 400 flat, hot-rolled steel panels from the same batch of steel, having dimensions of 152 by 102 by 3.2 mm, were grit blasted to SSPC SP-5, white metal finish, with a roughness profile of 50 to 70 mm.<sup>(14)</sup> After grit blasting, each panel was individually wrapped in moisture-resistant paper, which was not removed until the panel was ready to be coated.

#### Coated Panels

The 400 panels were randomly divided into 2 groups of 200 panels. Each group was coated with a different one-part commercial powder epoxy coating. (Hereinafter, these coatings are designated as Coating 1 and Coating 2.)

The coatings were applied on the customized line of a rebar coating plant. In this process, the steel panels were heated to 214 °C for 11 min, electrostatically sprayed with an epoxy powder coating, and then cured at 204 °C for 11 min. An attempt was made to control the thickness of the powder coating by controlling the number of times that the electrostatic gun was passed over a panel. This practice did not prove to be effective as will be evident from the discussion on coating thickness.

The coated panels were tested for holidays using a 67.5-V holiday detector equipped with a sponge attachment. Only four panels contained holidays and they were not used in this study.

The thickness of the coating on each panel was measured at five locations using an electromagnetic induction thickness gauge (at the locations marked with an "x" in figure 1). The within- and between-panel thickness variations were very large. In an effort to minimize the effect of thickness variation, two criteria were imposed. The first criterion was that the standard deviation for within-panel coating thicknesses had to be less than or equal to 25 mm. The second criterion was that the average coating thickness between panels had to fall within the range of 92 and 152 mm for the thin panels and within the range of 153 to 270 mm for the thick panels. Of these panels, 160 satisfied these criteria (see table 1). Approximately 20 of the remaining panels (that is, the panels not included in the anodic corrosion experiment) were used in the disbondment experiment.

Table 1. Number of panels and the average and standard deviation of the thicknesses of the Coating 1 and Coating 2 panels assigned to the anodic growth experiment.

THICKNESS	COATING 1 (thickness units: mm)	COATING 2 (thickness units: mm)
Thin (92 to 152 mm)		
number of panels	40	40
average (std dev)	130 (10)	130 (10)
Thick (153 to 270 mm)		
number of panels	40	40
average (std dev)	185 (30)	190 (25)

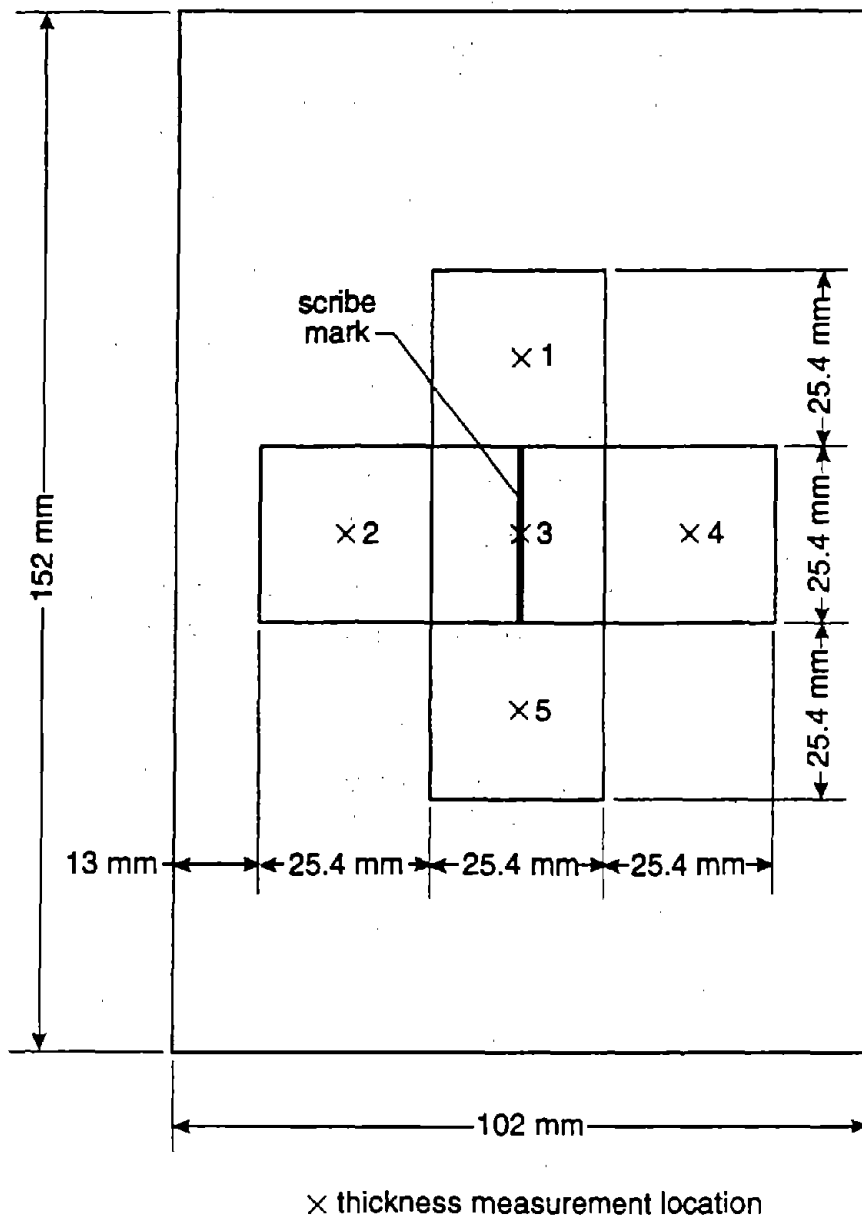


Figure 1. Location of thickness measurements for all panels being tested.

A one-way analysis of variance was performed at the 0.05 level of significance to determine if the mean thicknesses of the two coatings were significantly different. From this analysis, it was concluded that: (1) the average thicknesses of the thin Coating 1 and Coating 2 panels were not significantly different; (2) the average thickness of the thick Coating 1 and Coating 2 panels were not significantly different (the average thickness of the thin Coating 1 panels was significantly less than the average thickness of the thick Coating 1 panels); and, finally, the average thickness of the thin Coating 2 panels was significantly less than the average thickness of the thick Coating 2 panels.

Approximately 25 of the 40 panels in each thickness/coating group were scribed with a 25.4-mm by 1-mm scribe mark on a milling machine. As shown in figures 1 and 2, the scribe mark was located in the center of each panel; while for the disbondment panels, the scribe mark was located near the end of the panel (see figure 3). All scribe marks were visually inspected to ensure that no cracks or delaminations were present between the coating and the substrate.

A cylindrical ring of poly(methyl methacrylate) was bonded with a silicone adhesive to the top surface of each of the anodic growth panels. The silicone adhesive was allowed to cure for at least 2 weeks prior to filling the ring with the immersion solution (see next section). For the disbondment experiments, a rubber sealant was applied along the perimeter of each panel to contain the immersion solution (see Alsheh et al.).<sup>(15)</sup>

## **EXPOSURE ENVIRONMENT**

### **Immersion Solution**

The immersion solution was a saturated calcium hydroxide solution containing 3.5 percent by mass sodium chloride. The same immersion solution was used in both the anodic growth and the disbondment experiments.

### **Exposure**

Half (80) of the panels assigned to the anodic growth experiment were heated to  $35 \pm 1$  °C; while the other half were heated to  $50 \pm 1$  °C. The disbondment experiment was only conducted at  $35 \pm 1$  °C.

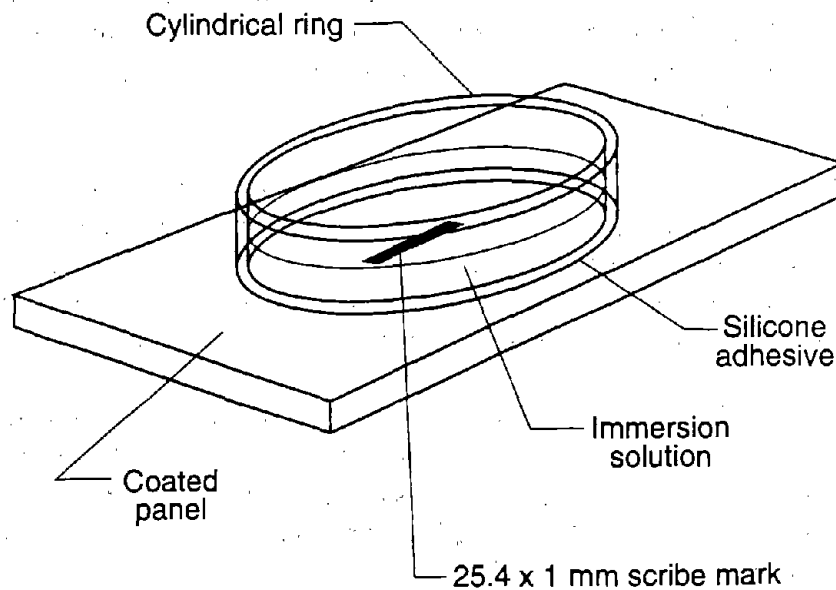
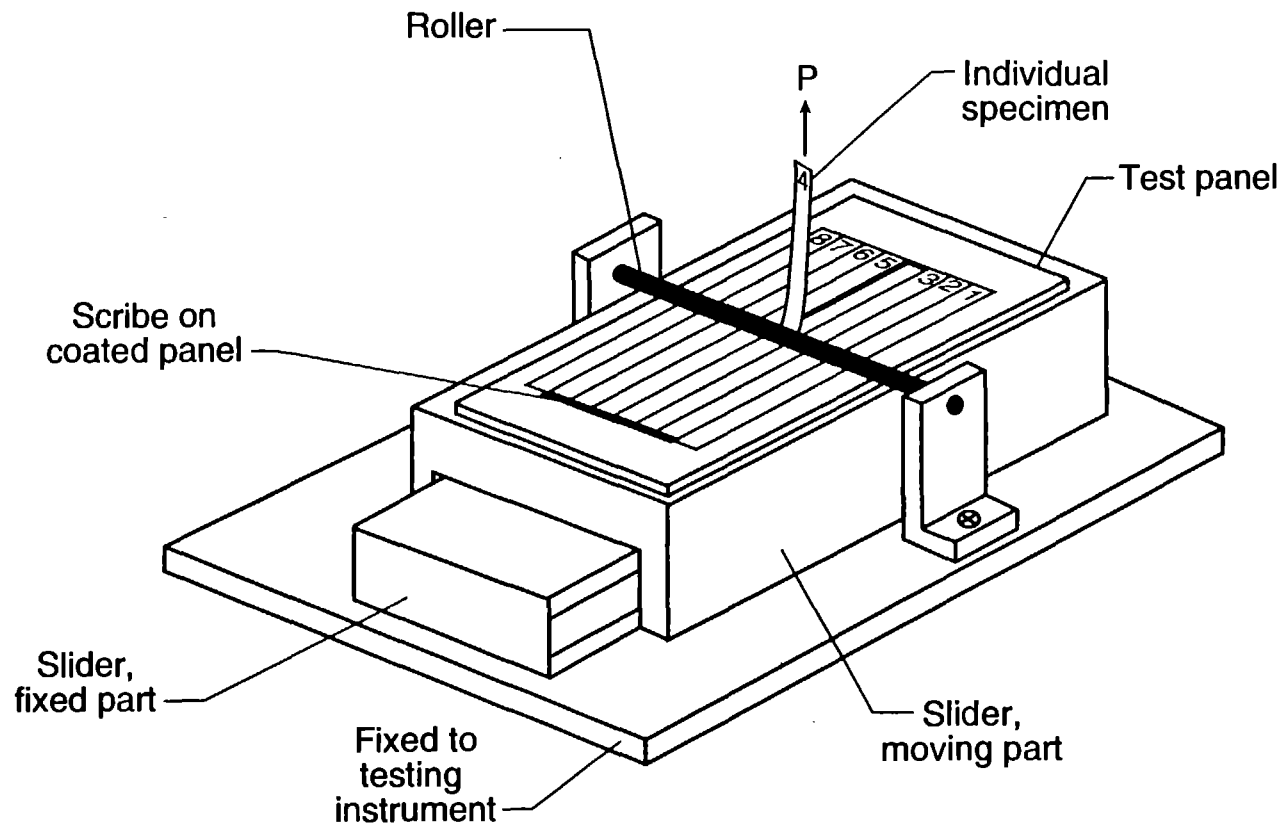


Figure 2. Schematic of experimental apparatus used in anodic growth studies.

In both experiments, the immersion solution was continuously aerated by bubbling filtered and desiccated air through it. Carbon dioxide in the air slowly neutralizes calcium hydroxide through a process called carbonation, causing a gradual reduction in the pH of the immersion solution. To control the effects of carbonation, the immersion solution was changed weekly for the 50 °C immersion experiment and once every 2 weeks for the 35 °C immersion experiment. Frequent measurement of the immersion solution indicated that its pH was maintained between 11.8 and 12.3. The concentration of oxygen within the immersion solution was also periodically monitored using an oxygen electrode. The concentration averaged  $7 \pm 0.2$  ppm by volume over the experimental period. The uncertainty is a standard deviation.



8

Figure 3. Peel test apparatus for measuring: (1) wet adhesion and (2) the progress of cathodic disbondment.



## FREE FILMS

In addition to the coated panels, free films of both coatings were prepared using the following procedure. A polished brass panel was sprayed with polytetrafluoroethylene release agent and then heated in an oven for 4 h at 200 °C to volatilize residual solvents and to improve the adhesion of the polytetrafluoroethylene to the substrate. The sprayed panels were then coated with the two epoxy powder coatings on the same customized line used in coating the other panels. After the coatings were cured, the free films were removed from the brass substrate by applying a slight thumb pressure to the coating.

A number of physical properties of the free films were measured, including glass transition temperatures, tensile strengths, tensile moduli, maximum elongation to break, and maximum moisture contents of Coatings 1 and 2. The glass transition temperatures were determined using a differential scanning calorimeter set at a scanning rate of 10 °C/min. The wet and dry tensile properties were measured in a testing machine at a crosshead speed of 2 mm/min. The tensile properties of the dry free films were measured after exposure at room conditions ( $23 \pm 1$  °C and  $50 \pm 2$  percent relative humidity) for 4 weeks. The wet tensile properties were measured after immersing the free films in pH 8 water for 2 weeks at  $35 \pm 0.5$  °C. The maximum moisture content of the free films was gravimetrically determined by immersing the free films in pH 8 water for 3 weeks at  $35 \pm 0.5$  °C. It was noted that the moisture content of the free films attained a maximum value after approximately 4 d of immersion. In addition, moisture permeability measurements were made based on ASTM Method D1653, Test Method for Water Vapor Transmission of Organic Coating Films.<sup>(16)</sup>

## QUANTIFICATION OF DEGRADATION

Scribed epoxy powder-coated panels degraded in three ways: (1) anodic corrosion and blistering, (2) cathodic disbondment, and (3) wet-adhesion loss. The anodic and cathodic areas were quantified using the techniques described below.

## Anodic Corrosion

The total anodic area, the sum of the individual anodic areas within the 25- by 25-mm<sup>2</sup> field of view of the thermographic camera centered on the scribe mark, was quantified using the infrared thermographic technique<sup>1</sup> described in McKnight and Martin.<sup>(17)</sup> Anodic sites only formed next to the scribe marks so that only location 3 in figure 1, the 25.4- by 25.4-mm<sup>2</sup> field of view centered on the scribe mark, was inspected.

The infrared technique is based on the principle that the thermal properties of the anodic corrosion are significantly different from the non-corroded areas. Experimentally, differences in the thermal emissions from the coated panel are detected by heating the front of a coated panel with a hot airstream heated to  $73 \pm 1$  °C. The airflow rate of the hot airstream was also maintained at 0.001 m<sup>3</sup>/s. A typical thermographic image showing anodic sites along the scribe mark is presented in figure 4.

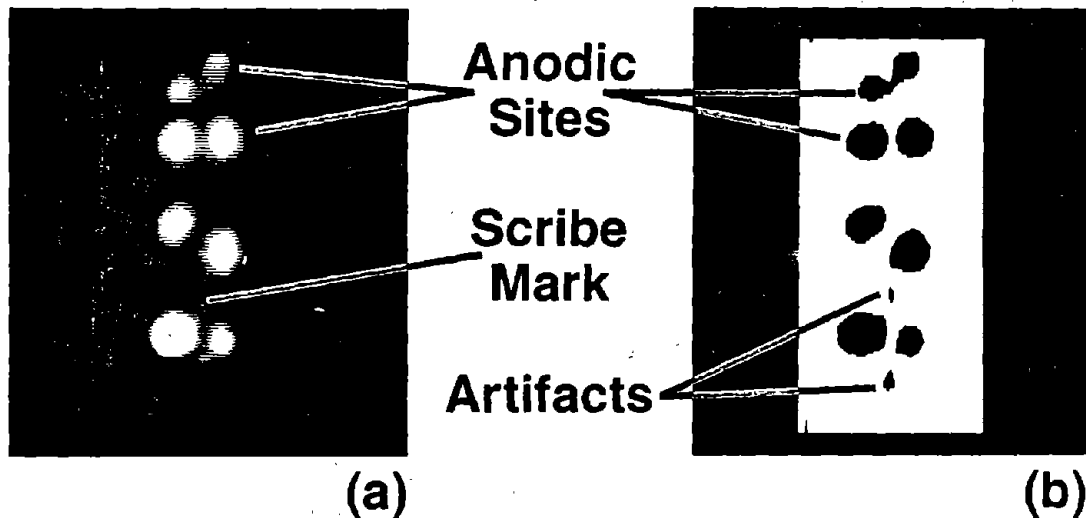


Figure 4. Thermographic image of the anode next to the scribe mark: (a) thermographic image and (b) computer-enhanced image..

---

<sup>1</sup>The thermographic technique is capable of measuring the size and location of each anodic site within the field of view.<sup>(17)</sup> For this study, the computer image processor attached to the thermographic camera was programmed to subtract the scribe mark from the image and to sum the contribution from all of the anodic sites within the 25- by 25-mm<sup>2</sup> field of view of the camera. That is, only the total anodic area was monitored.

## Elemental Analysis Through a Cross-Section of the Scribe

After 500 h of immersion at 35 °C, several panels were removed from the immersion solution and were cut in half through the scribe mark. This cross-section was analyzed by x-ray microanalysis to determine the spatial distribution of  $\text{Na}^+$ ,  $\text{Fe}^{++}$ ,  $\text{Cl}^-$ , and  $\text{Ca}^{++}$  ions through a cross-section of the scribe mark.

## Height and Compressive Strength of Anodic Blisters

Blisters began to form over the anodic sites between 500 and 1000 h after immersion in the solution at 35 °C and between 100 and 500 h at 50 °C. The height and compressive strength (a measure of the hydrostatic pressure of the fluid within the blister) of 20 of these anodic blisters were measured by compressing the blisters in a testing machine at a crosshead speed of 0.5 mm/min (figure 5). The height of each blister was measured with a micrometer.

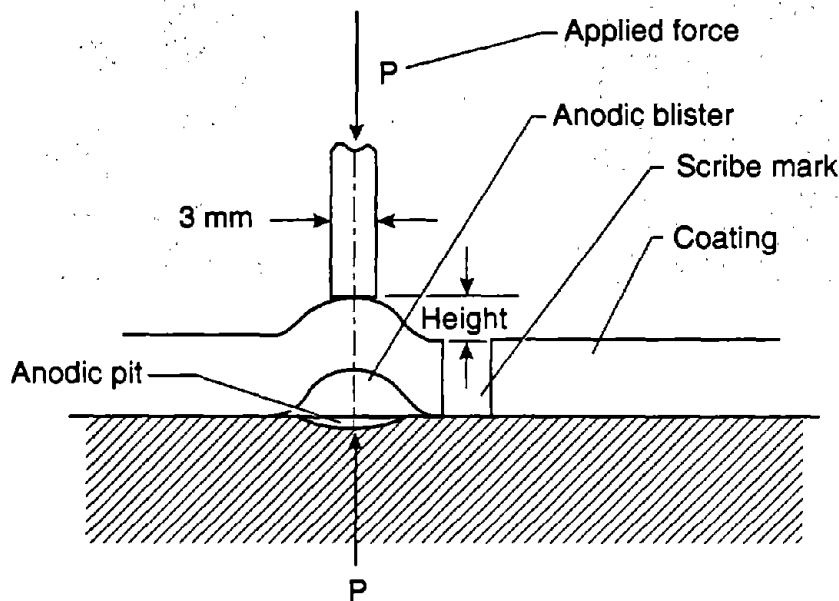


Figure 5. Anodic blister compression measurement.

## **Ion Concentrations and pH of Anodic Blister Fluid**

At the end of the immersion experiment, several of the blisters were lanced with a hypodermic needle and the fluid was removed. The pH and concentrations of  $\text{Na}^+$  and  $\text{Cl}^-$  ions in the blister fluid were determined using an ion-selective analyzer with pH and  $\text{Na}^+$  and  $\text{Cl}^-$  ion-selective microelectrodes.

## **Cathodic Disbondment and Wet-Adhesion Loss**

Disbondment, resulting from cathodic disbondment and wet-adhesion loss, was measured using the apparatus described in Alsheh et al. and shown in figure 3.<sup>(15)</sup> In this technique, the adhesion of the epoxy powder coating to the substrate was monitored while the coating was still wet from the water immersion using a  $90^\circ$  angle peel test. This technique did not work for dry coatings because the peel strength of the dry coatings was greater than the tensile strength and, thus, the coatings broke before peeling.

The protocol for making these measurements was as follows. A coated panel was removed from the immersion solution and immediately scribed with a standard razor blade into eight 10-mm-wide ribbons or specimens (see figure 3). While the coating was still wet, a portion of each specimen was carefully peeled from the substrate, starting at the end of the ribbon farthest from the scribe mark, leaving a length of approximately 40 mm of the specimen unpeeled. The panel was then positioned in a  $90^\circ$  peel apparatus consisting of a linear bearing slider fixed to a computer-controlled physical testing machine fitted with a recently calibrated 2000-g load cell. The peel test was conducted at room temperature and at a peel rate of  $20 \pm 0.1$  mm/min. The sliding friction of the apparatus was approximately  $40 \pm 2$  N/m.

## CHAPTER 3. RESULTS

### FREE FILMS

The physical properties of a coating system are often associated with its corrosion performance. Significant differences in the physical properties of Coatings 1 and 2 may indicate which properties of a coating system affect its corrosion performance. The physical properties of the two coatings are presented in table 2. The values reported are the average and standard deviations for five replicates.

One-way analysis of variance was performed to determine which properties of Coatings 1 and 2 were significantly different at the 0.05 level of significance. The glass transition temperature and dry and wet maximum elongation to break of Coating 1 were significantly greater than those of Coating 2; but the dry tensile strength and dry modulus of elasticity of Coating 1 were significantly less than those of Coating 2. The wet moduli of elasticity of Coatings 1 and 2 were not significantly different.

One-way analysis of variance was also performed to determine if the wet and dry properties within a coating type (that is, within Coatings 1 or 2) were significantly different at the 0.05 level of significance. For Coating 1, the dry and wet tensile strengths were not significantly different; but the wet tensile modulus of Coating 1 was significantly greater than its dry tensile modulus. The increase in the wet tensile modulus may have been due to plasticizer loss. For Coating 2, the dry tensile strength was significantly greater than the wet tensile strength and the dry tensile modulus was significantly greater than the wet tensile modulus.

### UNSCRIBED PANELS

Unscribed Coating 1 and Coating 2 panels were immersed in 35 °C immersion solution for 3072 h, during which none of the panels exhibited any visible sign of corrosion. The wet-adhesion peel strengths of two unscribed panels, one from each coating, were measured after 3072 h of immersion at 35 °C while the coatings were still wet. The wet-adhesion peel strength of Coating 1 was much greater than that of Coating 2. Coating 1 failed in tension prior to peeling. Knowing the applied tensile force at which Coating 1 failed, the equivalent peel force was computed. The wet-adhesion peel strength of Coating 1 was greater than 5.1 kN/m, while

Table 2. Physical properties of Coatings 1 and 2 free films.

PHYSICAL PROPERTY		COATING 1		COATING 2	
		average	std. dev.	average	std. dev.
Glass Transition Temp. (°C)		115	2	85	2
Tensile Strength (MPa)	dry	49.5	1.3	56.9	3.7
	wet	46.8	1.9	47.9	3.2
Tensile Modulus (GPa)	dry	1.37	0.03	1.71	0.17
	wet	1.55	0.13	1.69	0.17
Max. Elongation to Break(%)	dry	5.7	0.4	5.2	0.2
	wet	4.9	0.4	4.4	0.3
Max. Moisture Content (% by mass)		1.7	0.1	2.0	0.1

that of Coating 2 was 0.9 kN/m. The wet-adhesion peel strength of Coatings 1 and 2 were also measured after immersing unscribed coated panels in 80 °C immersion solution for 20 h. The wet-adhesion peel strength of Coating 1 was 0.5 kN/m, while that of Coating 2 was 0.17 kN/m.

Since none of the unscribed panels showed any sign of corrosion after 3072 h of immersion at 35 °C, a decision was made not to conduct the 50 °C unscribed immersion experiment. Instead, these panels were reassigned to the 35 °C disbondment experiment.

## SCRIBED PANELS

### Anodic Corrosion

Within 24 h of immersion, pitting corrosion sites (anodic sites) began to appear within 2 to 4 mm from the edge of the scribe marks in all of the scribed panels, regardless of the temperature of the immersion solution (see figures 4 and 6). (These pits were observed upon removal of the coating from the substrate of several panels.) Anodic sites appeared on some of the 35 °C panels within 5 h after immersion (the first inspection time) and within 2 h after immersion on some of the 50 °C panels. The coating was removed from several of the anodic sites, exposing a black pasty material that was believed to be magnetite,  $\text{Fe}_3\text{O}_4$ , similar to that observed for localized corrosion.<sup>(18)</sup> Indeed, when this material was dried, it displayed magnetic properties. The location of the black pasty material always corresponded to the size and location of the light spots in the thermographic image (see figure 4a). This black pasty material was scraped away, revealing a shallow pit that was assumed to be anodically induced.

For panels immersed in the 50 °C solution, the number and total area covered by the anodic sites on each panel were counted at each inspection; whereas, for the panels immersed in the 35 °C solution, only the total anodic area was determined. At 50 °C, the number of anodic sites did not change after approximately 100 h. The average number of anodic sites per panel for both Coatings 1 and 2, immersed in the 50 °C solution for 100 h, was 5.2 with a standard deviation of 1.5. Since the total anodic area increased, while the number of anodic sites (at least in the 50 °C immersion) remained constant after 100 h of immersion, the increase in total anodic area appears to be due to the growth of individual anodic sites.

Growth in the total anodic area,  $A(t)$ , obeyed the power law model having the form

$$A(t) = at^b$$

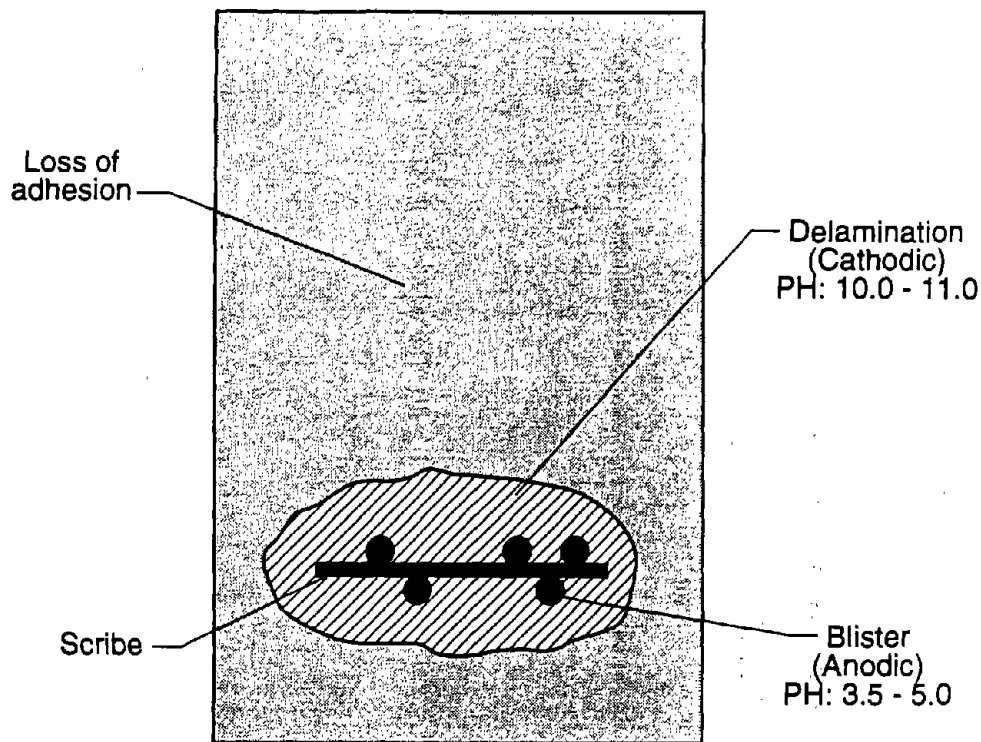


Figure 6. Location and shape of anodic sites next to scribe mark.

where  $t$  is the immersion time and  $a$  and  $b$  are constants. Figure 7a shows a typical fit of the power law model to the data. After taking the logarithms of both sides of the equation, a linear model was fit by least squares analysis. The power law coefficients and the squared correlation coefficient for the fit of the power law to anodic growth are tabulated in Appendix A for all of the panels placed on exposure. The  $a$  coefficient in Appendix A is, *of course*, the logarithm of the  $a$  in the above equation.

For a few panels in each temperature experiment, the power law model was not a good fit to the data. The entries for these panels are marked with an asterisk in the comments column in the tables in Appendix A. The power law model did not fit the data, either because anodic sites were present on the panel prior to the first inspection time or because the panel was removed from the experiment for chemical analysis after 500 h of immersion. For the panels in which anodes were present before the first inspection time, a straight line was a better fit to the data



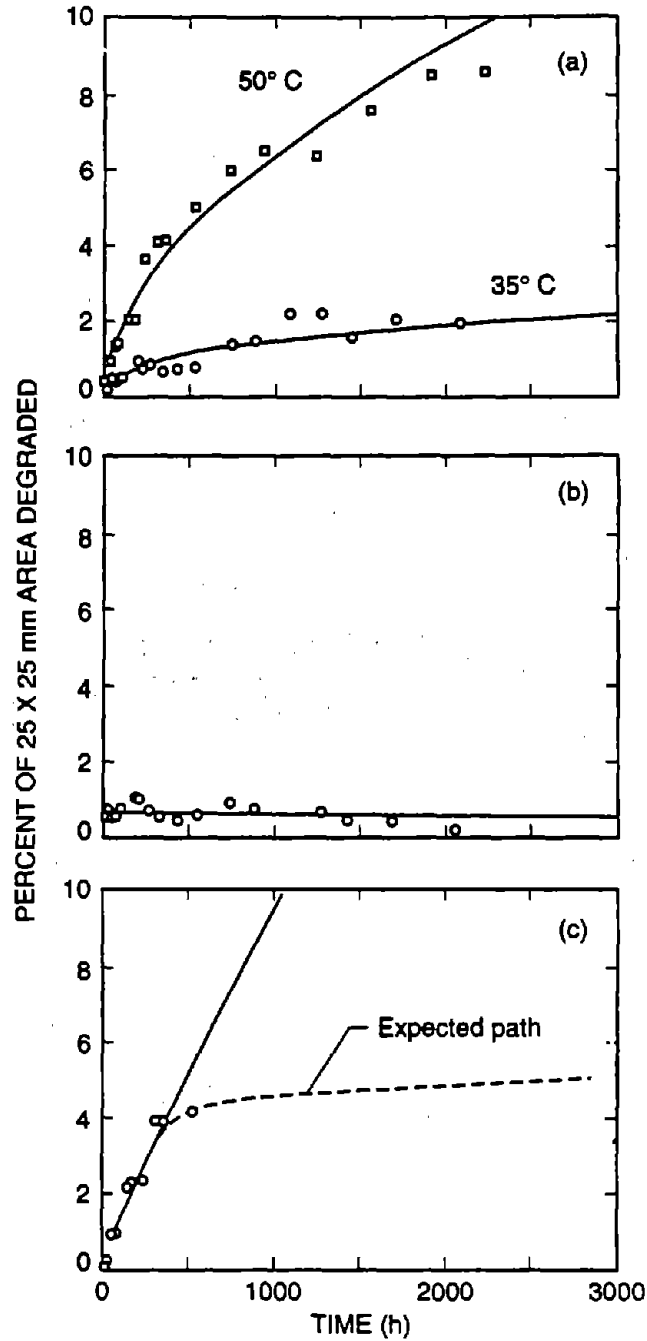


Figure 7. (a) Typical fits of the power law model to 35 and 50 °C total anodic area data as a function of immersion time, (b) straight line fit to panels in which anodic areas were present before the first inspection time, and (c) effect on the fit of the power law model when a panel was removed from the immersion experiment after 500 h.

than a power law model (see figure 7b); whereas for panels removed for chemical analysis, the power law model tended to overestimate the expected anodic growth response (see figure 7c). From Appendix A, it is obvious that substantial scatter exists in the values of the power law coefficients for panels exposed to the same experimental conditions. The large statistical scatter is consistent with observations made by Anderson.<sup>(19)</sup> For many of the panels, the data seemed to "heel over" more sharply than the power law model could accommodate—that is, the growth part of the curve looks like a power law, but at some point the curve levels out faster than the power law. Even so, considering the scatter in the data (especially for the 35 °C data, where the area being measured is small), the power law model fits the data reasonably well.

It is also worth noting that the two coefficients seem to be related from specimen to specimen. A plot of  $b$  versus  $a$  for the 35 and 50 °C specimens is presented in figure 8. The best fitting lines are  $b = (-0.063 - 0.171 a)$  and  $b = (0.184 - 0.136 a)$ .

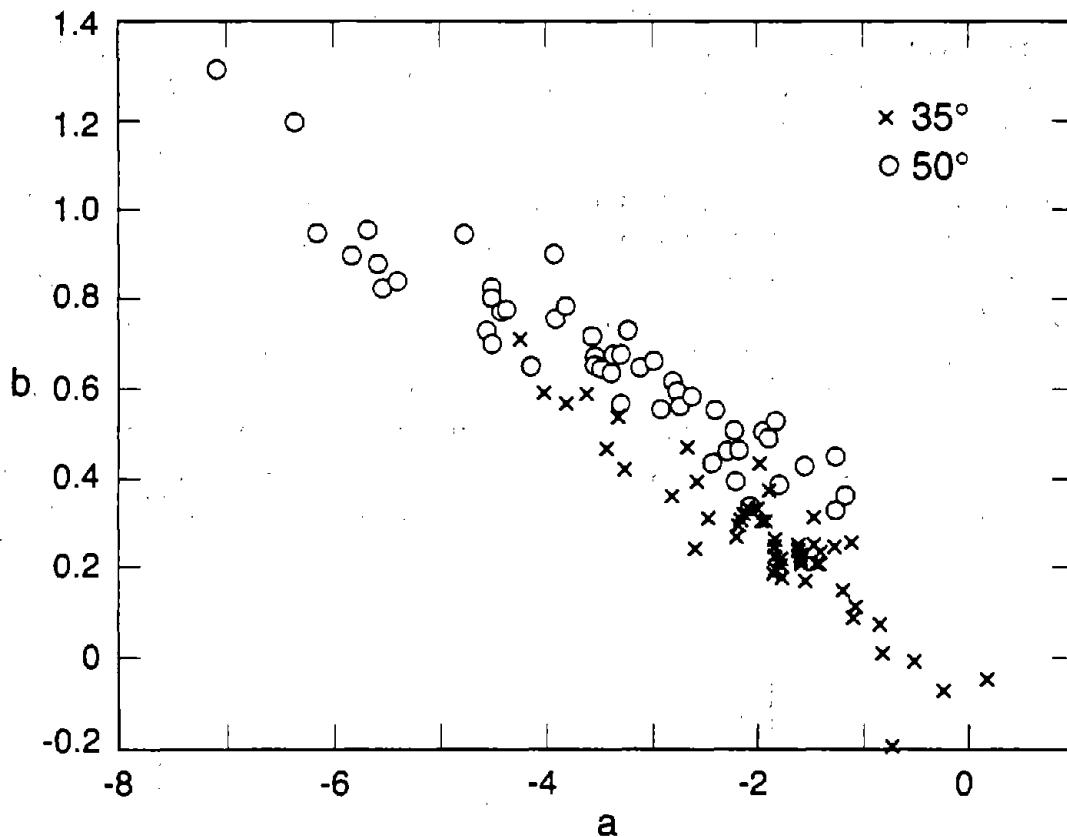


Figure 8. Plot of power law slope ( $b$ ) and intercept ( $a$ ) coefficients for 35 and 50 °C data.

A multifactor analysis of variance was performed to determine if coating type, coating thickness, or immersion temperature affected the value of the power law coefficients. It was concluded that the power law coefficients were not affected by coating thickness or coating type, but were significantly affected by immersion temperature. That is, an increase in the temperature of the immersion solution decreased the induction time for forming anodic sites and increased the total anodic area (see figure 7a).

After 500 h of immersion at 35 and 50 °C, blisters began to form above the anodes. The hydrostatic pressures in 20 of these blisters were measured after 2232 h of immersion by compressing the blisters. The average compressive stress for the 20 blisters tested was 0.84 MPa with a standard deviation of 0.42 MPa; while the average height of the blisters was 325 mm with a standard deviation of 200 mm.

Several of the anodic blisters were lanced with a hypodermic needle and the extracted fluid was characterized with respect to pH and  $\text{Na}^+$  and  $\text{Cl}^-$  ion concentrations. The pH of the blister fluid ranged from 5 to 5.5. The concentration of  $\text{Na}^+$  was about the same as in the bulk solution; whereas the concentration of  $\text{Cl}^-$  was three to six times greater than the concentration of  $\text{Cl}^-$  in the bulk solution. The anodic corrosion products within the blister fluid were mostly black pasty material that was presumed to be  $\text{Fe}_3\text{O}_4$ .

Elemental distributions of Cl, Na, Ca, and Fe were studied through a cross-section of the scribe mark and anodic blister area using a scanning electron microscope equipped with an x-ray microanalyzer. The results from this analysis are displayed in figure 9 for a cross-section near the scribe mark. The scribe mark is located on the right-hand side of each elemental map (it is easiest to see in the Fe distribution map (bottom row, far right)). The anodic site is the light-colored area next to the scribe mark and it contains a substantial amount of corrosion products. The Cl map (top row, far left) shows that chloride ions are present in the scribe mark and at the anodic site. The Ca map (bottom row, left) indicates that Ca is confined to the scribe mark. A small amount of Na (top row, middle) was observed at the scribe mark, but not within the anodic area.

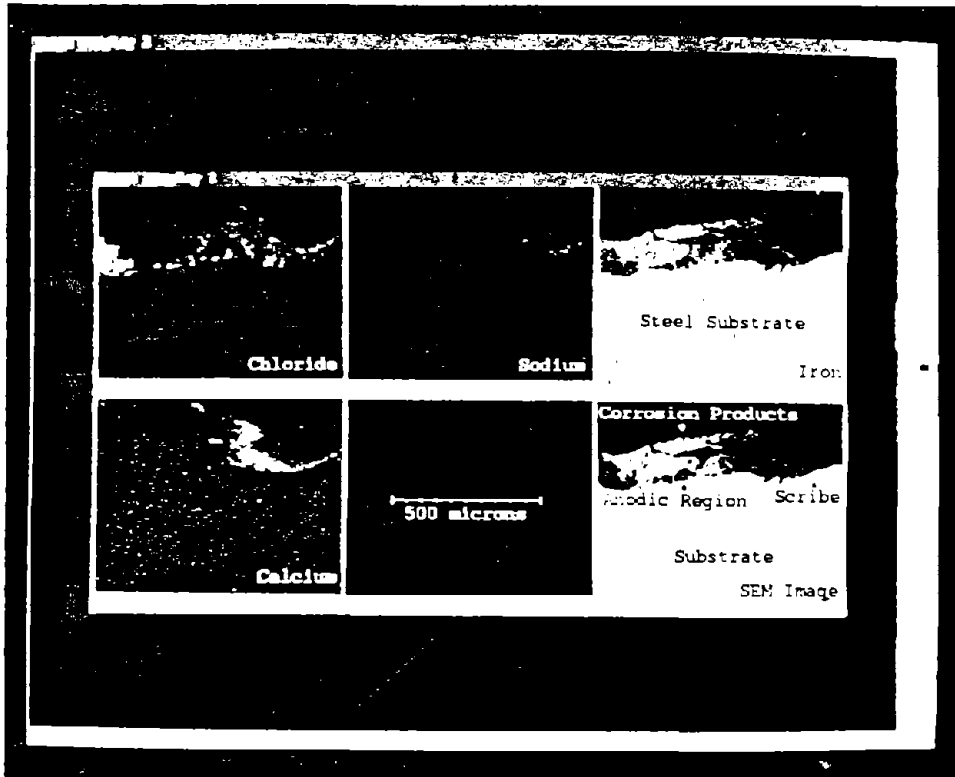


Figure 9. Elemental distribution maps through a cross-section near the scribe mark of a powder epoxy-coated steel panel. (Elemental maps include the scribe mark and an anodic site on the left-hand side of the scribe mark.)

### Cathodic Disbondment

Over the duration of the 35 and 50 °C experiments, the scribe marks remained free of corrosion products. That is, the scribe acted like a cathode. After approximately 500 h of immersion at 35 °C, the bond strength of the coating to the substrate immediately surrounding the anodic sites had fallen to a point where the coating could be easily removed from the substrate. This loss in bond strength was attributed to cathodic disbondment.<sup>(20-24)</sup> The disbonded<sup>2</sup> area increased with immersion time. To verify that the disbonded area was cathodic,

<sup>2</sup>The term "disbonded" is used in describing the loss in bond strength of the coating to the substrate resulting from cathodic disbondment. This terminology is not precise, however, in that the coating was not completely detached from the substrate.

the coating was removed from the substrate and the pH of the steel substrate underneath the disbonded coating was determined to be greater than 10. X-ray microanalysis (see figure 9) showed trace amounts of sodium ions on the steel surface; calcium and chloride ions, however, were not detected.

The initial stages of cathodic disbondment could not be followed, since peel measurements could only be made after the force required to peel the coating from the substrate was less than the force required to fail the coating film in tension. In figure 10, the peel strength curves for Coating 2 are plotted against distance from the scribe mark after various immersion times. In figure 11, the disbonded distance (the distance between the scribe mark and the disbondment front) is plotted against immersion time. The maximum disbonded distance increased linearly for the first 50 d of immersion, after which the rate of disbondment decreased. The rate of disbondment was not affected by coating thickness.

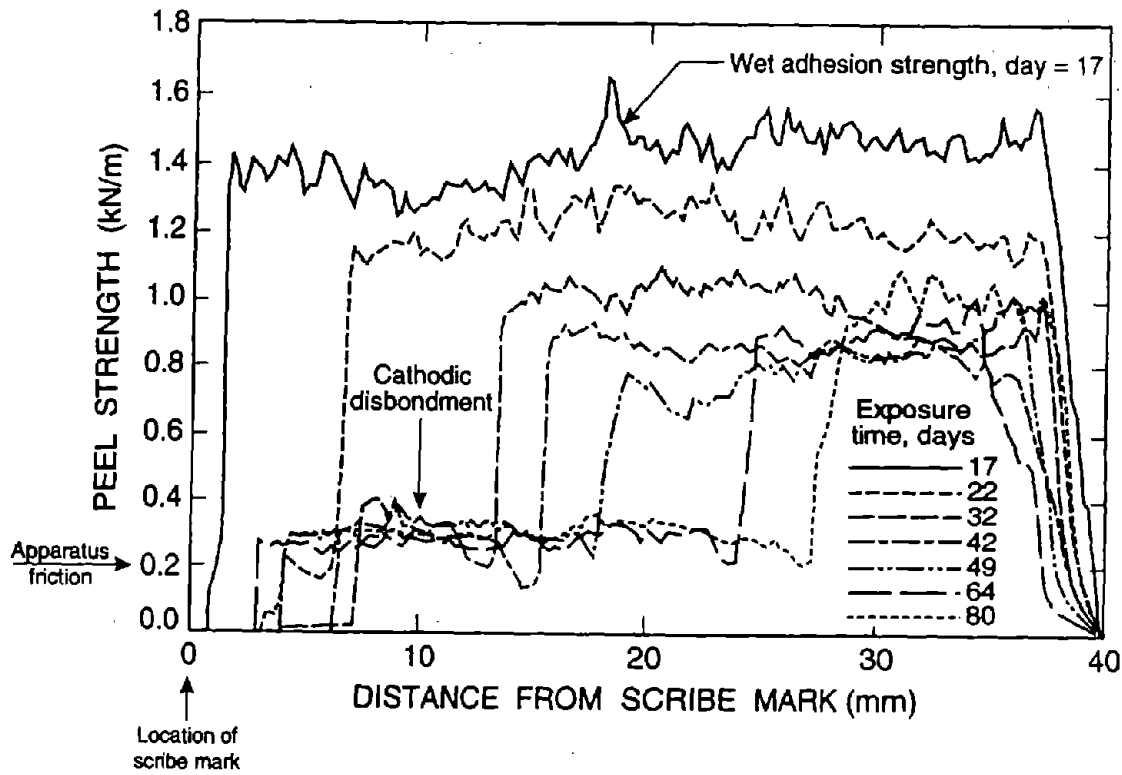


Figure 10. Peel strength as a function of distance from the scribe mark for coated panels immersed for different periods of time (taken from Alsheh et al.).<sup>(15)</sup>

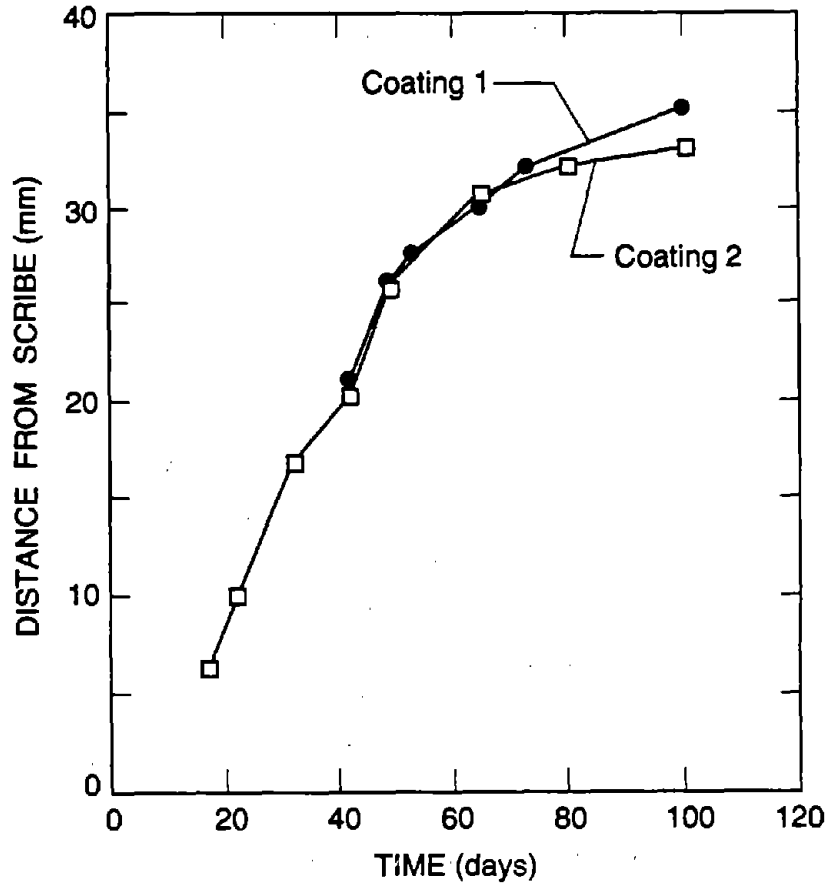


Figure 11. Maximum disbonded distance from the scribe mark as a function of immersion time (taken from Alsheh et al.).<sup>(15)</sup>

### Wet-Adhesion Loss

Loss in bond strength beyond the cathodic disbondment front was attributed to wet-adhesion loss, resulting from the accumulation of water molecules between the coating and the substrate.<sup>(24-28)</sup> This was tested on unscribed continuously immersed panels. The loss in wet-adhesion peel strength of these panels reached a constant value after approximately 42 d of immersion (see figure 12).

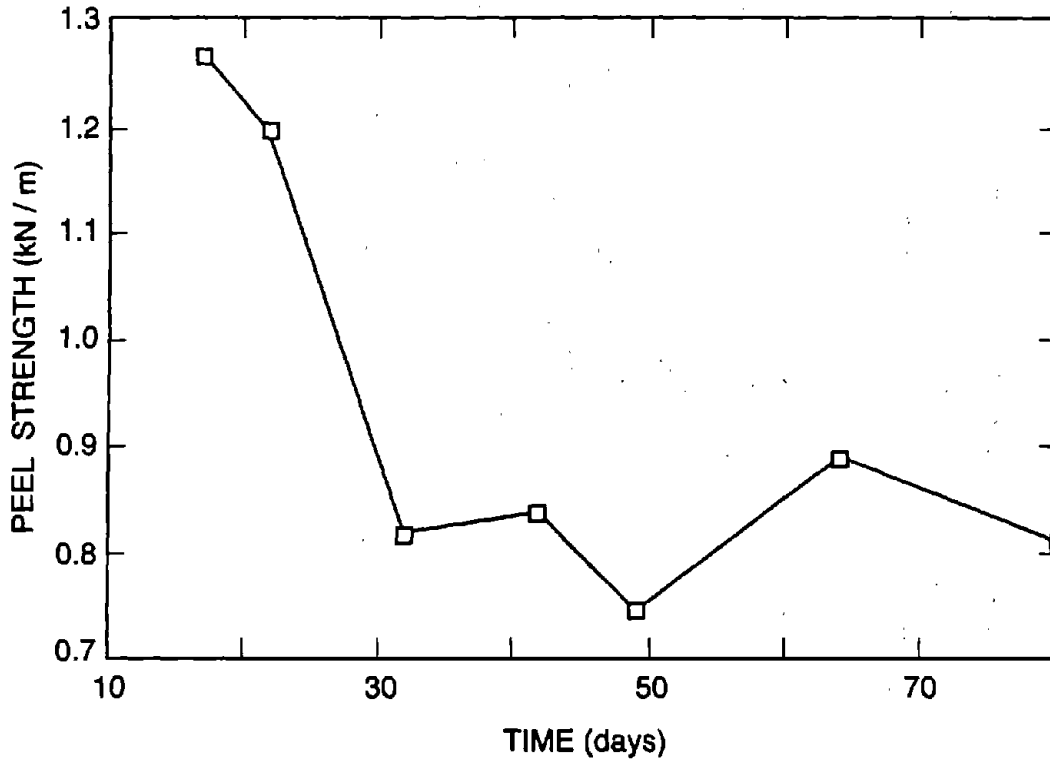


Figure 12. Wet-adhesion strength loss versus immersion time.

Unlike cathodic disbondment, wet-adhesion loss should be recoverable once the coating is dried. To demonstrate this, several unscrubbed panels were immersed in the immersion solution at 35 °C for 3 weeks, removed from the solution, and allowed to dry at room conditions ( $24 \pm 2$  °C and  $45 \pm 3$  percent relative humidity). The wet-adhesion peel strength of the coating to the substrate for the first panel was measured immediately after removal from the solution. On successive days, another panel was randomly selected and its bond strength measured. Figure 13 shows this recovery. This experiment was terminated after 13 d, at which time the peel strength was 1.2 kN/m. This value is about 20 percent of the load required to fail the dry free films, which failed in tension at 5.1 kN/m. None of these panels exhibited any corrosion.

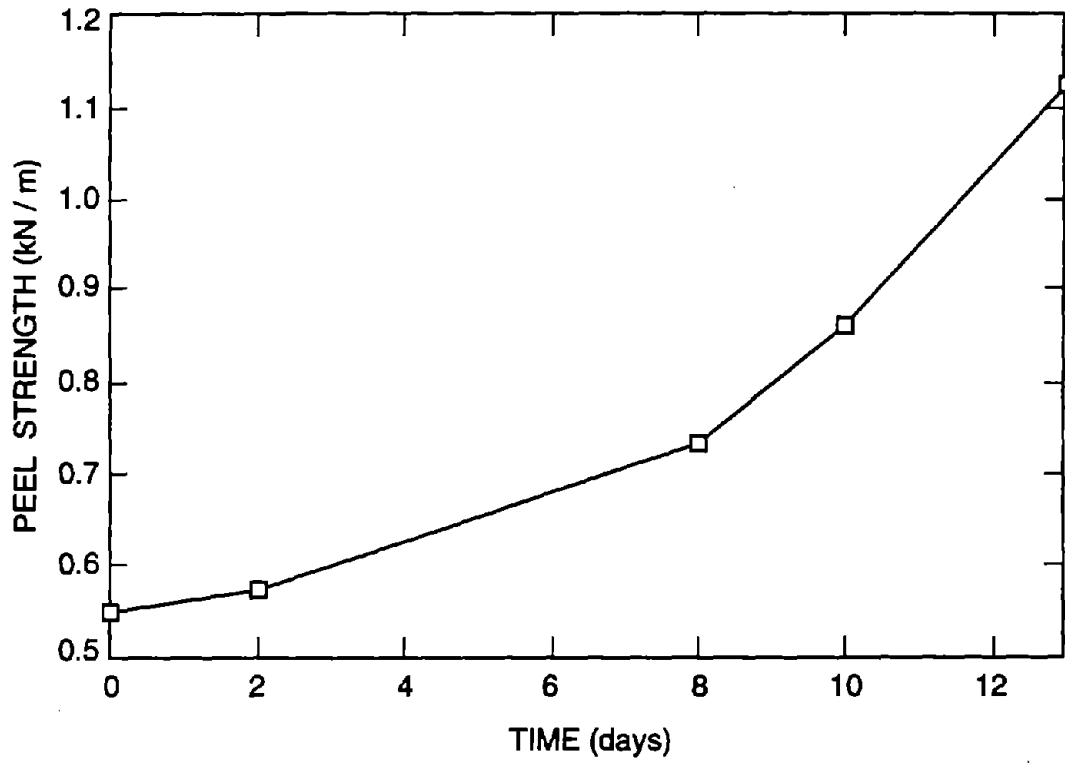


Figure 13. Wet-adhesion strength recovery as a function of drying time.



## CHAPTER 4. DISCUSSION

### UNSCRIBED PANELS

The diffusivity of chloride and sodium ions through intact coatings is known to be very low and, thus, the rates of corrosion of the epoxy powder-coated steel panels must be expected to depend largely on the presence or absence of defects through the thickness of the coating.<sup>(29,30)</sup> In our experiment, the unscribed coated panels did not corrode after 3072 h of immersion at 35 °C; whereas scribed coated panels began to corrode within 5 h after immersion at 35 °C.

### SCRIBED PANELS

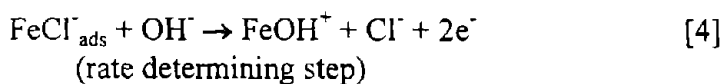
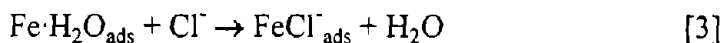
#### Anodic Corrosion

The formation of the anodic sites on the scribed panels is consistent with crevice corrosion processes.<sup>(31-33)</sup> This is a localized corrosion process in which  $\text{Cl}^-$  ions migrate through separations in the coating/substrate interface and form an anodic site at a location underneath the coating at which the pH of the interfacial liquid is low enough to support corrosion.<sup>(24)</sup>

The main cathodic reaction in crevice corrosion in a neutral solution is the reduction of oxygen:<sup>(34,35)</sup>

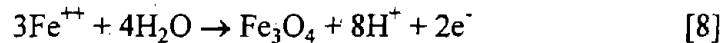
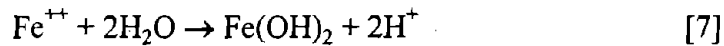
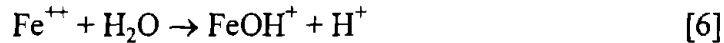


while the principal anodic reactions include:<sup>(35)</sup>

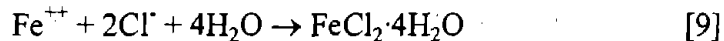


The net result of the anodic reactions is the production of electrons and  $\text{Fe}^{++}$  ions. From our experimental results, the  $\text{Cl}^-$  (Reaction 4) migrated between 2 and 4 mm from the scribe mark before an anodic site was established. The net result of the cathodic reaction (Reaction 1) is the production of an excess of hydroxide ions that eventually leads to cathodic delamination.

The  $\text{Fe}^{++}$  ions produced in Reaction 5 are hydrolyzed with acidification, according to any of the following possible reactions:<sup>(18,36)</sup>



In the absence of oxygen, Reaction 8 is thermodynamically favored.<sup>(18)</sup> The depletion of oxygen further decreases the pH in the anodic site. With the buildup of  $\text{Fe}^{++}$  and  $\text{H}^+$  ions within the confined local electrolytes, negatively charged ions are required to preserve electrical neutrality. These negative ions are believed to be supplied by  $\text{Cl}^-$  transported along the coating/substrate interface from the bulk solution, since  $\text{Cl}^-$  ions are more abundant in the bulk solution than are the  $\text{OH}^-$  ions. McCafferty suggested that the resulting increased local concentration of ferrous chloride is limited by the following reaction:<sup>(36)</sup>



These processes account for the presence of the large quantity of chloride in the anodic blisters, as observed in figure 9.

After 500 h of immersion, the concentration of  $\text{Cl}^-$  within the anodic blisters (measured with a chloride electrode) began to exceed the concentration of  $\text{Cl}^-$  ions in the bulk solution.  $\text{Cl}^-$  ions migrate toward the anodic sites under the influence of an electrical potential gradient through a process commonly called electro-osmosis or electroendosmosis.<sup>(33,37-39)</sup> Once the  $\text{Cl}^-$  ion concentration at the anode exceeded the bulk  $\text{Cl}^-$  ion concentration, water was transported into the anodic area under a solute concentration gradient.

As more and more water was transported to the anodic site, an anodic blister was formed. This blister continued to grow until an equilibrium was established between the electrical potential and solute gradients, and the elastic stresses in the wet coating tended to force water and  $\text{Cl}^-$  ions out of the blister.<sup>(39)</sup> From microelectrode measurements, the concentration of  $\text{Cl}^-$  in the anodic blister fluid was from 4 to 6 times greater than the  $\text{Cl}^-$  concentration in the bulk solution. Ritter and Rodriguez reported chloride concentrations 3 to 4 times greater than in the bulk solution, while Nguyen and Lin reported  $\text{Cl}^-$  concentrations that were 10 times greater

than in the bulk solution.<sup>(40,41)</sup> The bulk solutions in these experiments, however, were neutral. Increasing the temperature of the immersion solution from 35 to 50 °C caused the blisters to increase in size. This was expected since it is known that the elastic moduli of the coatings decrease, while the rate of transport of ions increases with an increase in temperature.

### **Cathodic Disbondment**

In all corrosion processes, an electronic balance is established between the growth of the anodic and cathodic regions. Thus, as the anodic activity increases, the cathodic area must also increase through a process called cathodic disbondment.<sup>(20-24,42)</sup> In cathodic disbondment, hydroxide ions produced in Reaction 1 cause disbondment of the coating from the substrate (thus, the name cathodic disbondment). In neutral chloride environments (where the pH of bulk electrolyte is 7), the pH of the disbonding solution at the delamination front has been reported to be as high as 14.<sup>(43)</sup> However, most pH measurements are integrated over a large volume of liquid and, thus, the pH values commonly reported in the literature are closer to 10 (see citations in Leidheiser et al.; Martin et al.), which was the pH value in this experiment.<sup>(21,44)</sup> The alkalinity of the disbonding fluid is normally attributed to sodium hydroxide (NaOH), since a strong base is required to separate the coating from its substrate (calcium hydroxide is too weak an alkali to delaminate a coating from its substrate).<sup>(21,42)</sup> Support for sodium hydroxide being the disbonding agent was also provided by x-ray microanalysis of the steel substrate in which sodium ions were found in the disbondment areas, but not calcium ions (see figure 9). The independence of the rate of cathodic delamination and thickness of the coating is consistent with the results reported by Leidheiser et al.<sup>(21)</sup>

### **Wet-Adhesion Loss**

Bond strength is also lost due to the buildup of water molecules at the interface between Coating 2 and the substrate through a process called wet-adhesion loss.<sup>(25,26,28)</sup> (The wet-adhesive strength of panels coated with Coating 1 immersed at 35 °C could not be measured with the apparatus shown in figure 3, because the coating failed in tension instead of peeling from the substrate.) Wet-adhesion loss is commonly observed in coatings adhering to a high-energy substrate, such as steel, that are exposed to high relative humidity or moist environments. From figure 12, it appears that the wet-adhesion losses for Coating 2 reached a constant value after 30 d of immersion. Also, most of the wet-adhesion loss experienced by Coating 2 during immersion appears to be recoverable when the coated panels are allowed to dry (figure 13).

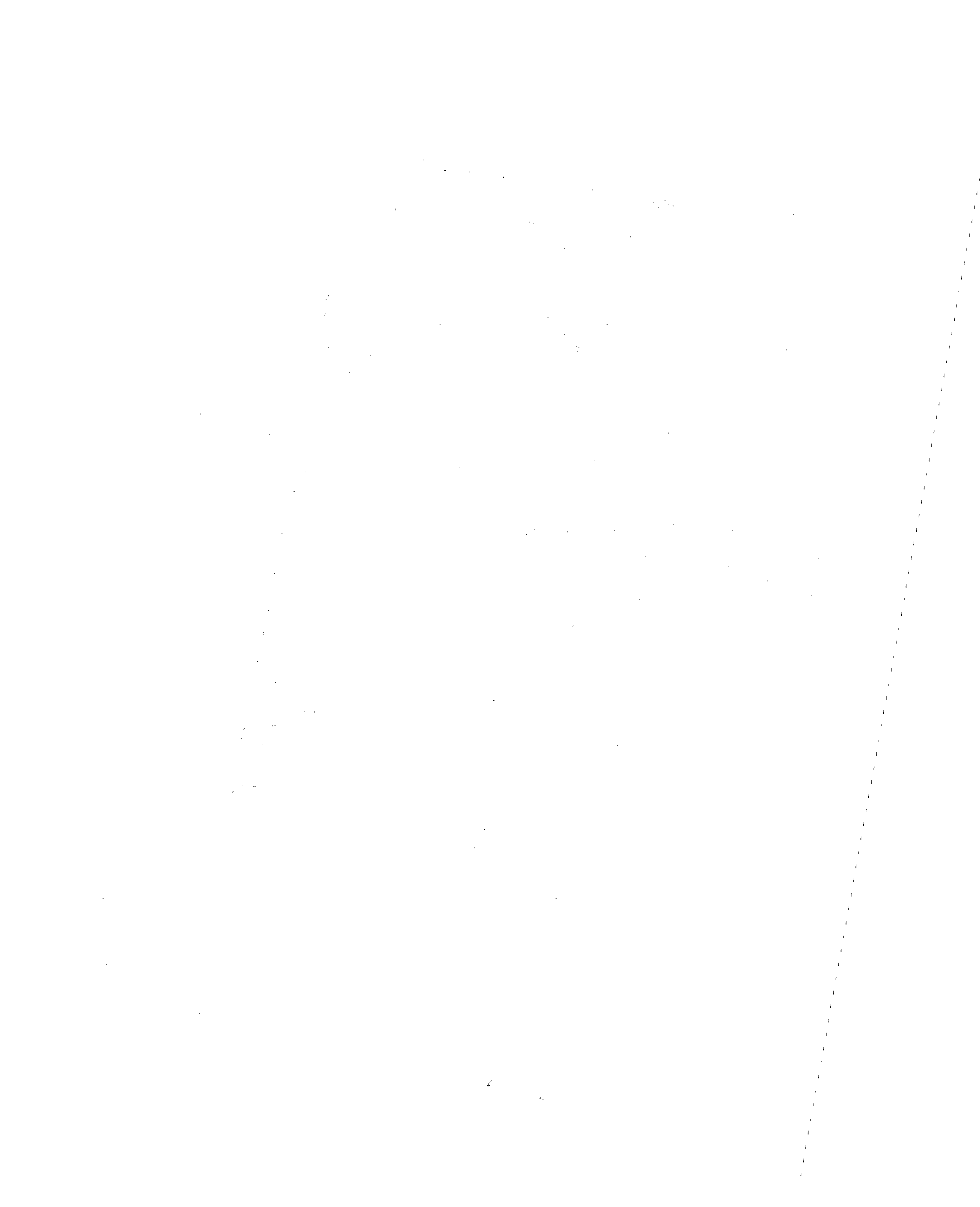
Funke's assertion that the wet-adhesion strength of a coating is the most important factor for determining a coating's corrosion performance was not supported by our experimental results<sup>3 (24)</sup>. Thus, even though the wet-adhesion strength of Coating 1 was at least 5 times greater than the wet-adhesion strength of Coating 2 when immersed in the 35 °C immersion solution, and over 2-1/2 times greater than Coating 2 when immersed in the 80 °C immersion solution, the anodic and cathodic disbondment growth rates for the two coatings were not significantly different. It should be noted, however, that the conclusions of Funke were based on experiments in which coated panels were immersed in a neutral solution, whereas our experiments were conducted in a strongly alkaline solution.<sup>(24)</sup>

---

<sup>3</sup>Correspondingly, our results support Walker's assertion that wet-adhesion strength is not a primary determinant of a coating's corrosion protection performance.<sup>(25,26)</sup>

## CHAPTER 5. CONCLUSIONS

1. None of the unscribed panels corroded after 3072 h of immersion at 35 °C; while all of the scribed panels started to corrode within 24 h of immersion at both 35 and 50 °C.
2. An increase in the temperature of the immersion solution from 35 to 50 °C greatly accelerated the rate of corrosion of the scribed panels.
3. After 500 h of immersion at 35 °C (between 100 and 500 h at 50 °C), liquid-filled blisters formed above each anodic site. The chloride ion concentration of the blister fluid was four to six times greater than that of the bulk electrolyte.
4. Bond strength of the coating to the substrate was lost through cathodic disbondment and wet-adhesion loss.
5. The rate of cathodic disbondment was not affected by coating type or coating thickness, but it was greatly affected by an increase in temperature of the immersion solution.
6. Wet-adhesion loss was not affected by coating thickness, but it does depend on coating type and immersion temperature. Even though the wet-adhesion strength of the two coatings differed by a factor of five, however, the rate of corrosion for the two coatings was not significantly different.



## APPENDIX A. POWER LAW GROWTH OF ANODIC AREA

Table 3. Coefficients of the power law model.  
(a) Coating 1, scribed panels immersed in the immersion solution at 35 °C.

Coating	Thickness	Spec No.	a	b	r <sup>2</sup> (%)	Comment
1	thin	1	-1.89	0.23	64	
1	thin	14	-4.11	0.62	72	
1	thin	25	-1.37	0.26	87	
1	thin	30	-2.04	0.40	92	
1	thin	39	-2.57	0.34	48	
1	thin	49	-1.71	0.27	76	
1	thin	59	-3.42	0.56	81	
1	thin	60	-2.31	0.30	64	
1	thin	62	-3.38	0.45	60	
1	thin	63	-1.96	0.22	60	
1	thin	66	-1.18	0.14	42	
1	thin	67	-1.70	0.26	87	
1	thin	76	-1.74	0.26	73	
1	thick	7	-1.53	0.23	76	
1	thick	7a	-2.70	0.27	40	
1	thick	9	-1.63	0.22	79	
1	thick	18	-1.88	0.21	53	
1	thick	28	-1.94	0.24	40	
1	thick	34	-1.71	0.24	76	
1	thick	44	-0.93	0.04	5	*straight line
1	thick	60	-0.63	0.02	6	*straight line
1	thick	61	-1.02	0.11	16	
1	thick	66	-0.85	-0.15	5	*straight line
1	thick	73	-1.66	0.20	49	
1	thick	78	-2.29	0.32	57	
1	thick	79	-1.56	0.23	76	

\*Power law model was not a good fit to the data.

Table 3. Coefficients of the power law model (continued).  
 (b) Coating 2, scribed panels immersed in the immersion solution at 35 °C.

Coating	Thickness	Spec No.	a	b	r <sup>2</sup> (%)	Comment
2	thin	1	-2.24	0.33	83	
2	thin	7	-0.35	-0.04	3	*straight line
2	thin	9	-1.58	0.28	79	
2	thin	19	-2.06	0.46	94	
2	thin	31	-1.85	0.26	74	
2	thin	35	-0.99	0.22	75	
2	thin	37	-1.34	0.27	67	
2	thin	45	-1.50	0.26	89	
2	thin	46	-4.32	0.74	81	
2	thin	48	-2.77	0.49	82	
2	thin	58	-2.20	0.35	94	
2	thin	59	-3.46	0.48	51	
2	thin	82	-2.25	0.35	78	
2	thick	10	-2.25	0.34	74	
2	thick	16	-1.95	0.29	77	
2	thick	20	-1.88	0.24	83	
2	thick	21	-1.31	0.18	73	
2	thick	38	-3.63	0.59	63	*straight line
2	thick	39	-1.20	0.12	48	
2	thick	40	-2.69	0.42	85	
2	thick	48	-1.94	0.26	61	
2	thick	52	-3.91	0.60	71	
2	thick	57	0.06	-0.01	2	*straight line
2	thick	63	-2.04	0.33	84	*truncated data
2	thick	67	-2.12	0.36	87	
2	thick	80	-2.90	0.39	79	

\*Power law model was not a good fit to the data.



Table 3. Coefficients of the power law model (continued).  
(c) Coating 1, scribed panels immersed in the immersion solution at 50 °C.

Coating	Thickness	Spec No.	a	b	r <sup>2</sup> (%)	Comment
1	thin	5	-2.51	0.45	89	
1	thin	8	-5.88	0.92	86	
1	thin	21	-5.76	0.97	91	
1	thin	21a	-2.28	0.52	98	
1	thin	22	-4.40	0.79	80	
1	thin	23	-1.62	0.44	94	
1	thin	26	-1.24	0.37	94	
1	thin	27	-4.58	0.84	94	
1	thin	32	-4.52	0.79	86	
1	thin	40	-6.39	1.19	88	*truncated data
1	thin	56	-1.33	0.34	96	
1	thin	61	-3.59	0.66	78	
1	thick	4	-5.46	0.85	90	
1	thick	6	-2.49	0.57	98	
1	thick	19	-7.10	1.31	95	*truncated data
1	thick	30	-4.19	0.67	89	
1	thick	38	-4.59	0.82	94	
1	thick	45	-5.60	0.84	95	
1	thick	53	-4.67	0.76	81	
1	thick	63	-3.35	0.58	90	
1	thick	67	-3.51	0.66	91	
1	thick	76	-2.14	0.34	86	
1	thick	80	-1.86	0.39	93	
1	thick	82	-6.22	0.97	88	
1	thick	85	-5.65	0.90	91	

\*Power law model was not a good fit to the data.

Table 3. Coefficients of the power law model (continued).  
 (d) Coating 2, scribed panels immersed in the immersion solution at 50°C.

Coating	Thickness	Spec No.	a	b	r <sup>2</sup> (%)	Comment
2	thin	1	-3.18	0.66	97	
2	thin	3	-2.86	0.62	95	
2	thin	11	-2.01	0.51	95	
2	thin	12	-2.71	0.60	96	
2	thin	13	-2.71	0.57	95	
2	thin	32	-3.92	0.89	97	*truncated data
2	thin	34	-1.30	0.46	94	
2	thin	44	-2.80	0.60	95	
2	thin	52	-3.96	0.76	94	
2	thin	71	-4.81	0.95	88	*truncated data
2	thin	73	-2.21	0.47	95	
2	thin	77	-1.89	0.54	98	
2	thick	5	-2.36	0.48	96	
2	thick	15	-3.33	0.68	95	
2	thick	21	-3.89	0.80	95	
2	thick	29	-3.01	0.67	95	
2	thick	31	-3.41	0.68	98	
2	thick	32	-3.59	0.68	96	
2	thick	43	-3.00	0.57	93	
2	thick	53	-4.58	0.73	86	
2	thick	55	-2.28	0.40	94	
2	thick	58	-3.43	0.65	82	
2	thick	59	-3.63	0.73	88	
2	thick	76	-2.22	0.48	94	
2	thick	79	-4.55	0.71	87	

\*Power law model was not a good fit to the data.

## REFERENCES

1. L.D. Sandvig, *Highway Builder*, November, 1974, pp. 16-17.
2. P.D. Cady, "Corrosion of Reinforcing Steel in Concrete—A General Overview of the Problem," *Chloride Corrosion of Steel in Concrete*, ASTM STP 629, D.E. Tonini and S.W. Dean [Eds.], American Society for Testing and Materials, 1977, pp. 3-11.
3. F.O. Wood, "Deicing Salt Usage in North America," *Proceedings of the National Association of Corrosion Engineers*, Paper No. 7, presented at the National Association of Corrosion Engineers meeting in March, 1978.
4. J.R. Clifton, H.F. Beeghly, and R.G. Mathey, *Nonmetallic Coatings for Concrete Reinforcing Bars*, Federal Highway Administration Report No. FHWA-RD-74-18, 1974.
5. T.L. Neff, "Letter to Specifiers of Corrosion Protection Systems," *Concrete Reinforcing Steel Institute*, February, 1992.
6. A.A. Sagüés, *Mechanism of Corrosion of Epoxy-Coated Reinforcing Steel in Concrete, Final Report*, Florida Department of Transportation Report No. FL/DOT/RMC/0543-3296, 1991.
7. J. Allen, "Epoxy-Coated Rebar Benefits Minnesota Deck," *Roads and Bridges*, 1993, June, p. 38.
8. D.F. Burke, "Performance of Epoxy-Coated Rebar, Galvanized Rebar, and Plain Rebar with Calcium Nitrite in a Marine Environment," *Proceedings of the International Conference on Corrosion and Corrosion Protection of Steel in Concrete*, University of Sheffield, England, July 24-29, 1994.
9. R.J. Kessler and R.G. Powers, *Interim Report on the Corrosion Evaluation of Substructure at the Long Key Bridge*, Florida Department of Transportation, Bureau of Materials and Research, Handout, July 13, 1988 (no report number).
10. L.L. Smith, R.J. Kessler, and R.G. Powers, "Corrosion of Epoxy-Coated Rebar in a Marine Environment," *Transportation Research Circular*, vol. 403, 1993, p. 36.
11. R.J. Kessler and R.G. Powers, *Corrosion of Epoxy-Coated Rebar: Keys Segmental Bridges, Monroe County, Florida*, Department of Transportation, Bureau of Materials and Research, Report No. 88-8A, 1988.

12. K.C. Clear, *Effectiveness of Epoxy-Coated Reinforcing Steel*, Kenneth C. Clear, Inc., Consulting Report, January 10, 1992.
13. K.C. Clear, "Effectiveness of Epoxy-Coated Reinforcing Steel (C-SHRP Report: Executive Summary)," *Transportation Research Circular*, vol. 403, 1993, p. 66.
14. Steel Structures Painting Council, "Surface Preparation Specification No. 5—White Metal Blast Cleaning," *Steel Structures Painting Manual, Volume 2, System and Specifications*, 6th edition, Pittsburgh, PA, 1985.
15. D. Alsheh, T. Nguyen, and J.W. Martin, "Adhesion of Fusion Bonded Epoxy Coatings on Steel in Alkaline Solution," *Proceedings of the Adhesion Society*, Orlando, FL, February, 1994.
16. ASTM, "Test Method for Water Vapor Transmission of Organic Coating Films (ASTM D1653)," *American Society for Testing and Materials*, vol. 6.01, ASTM, Philadelphia, PA, 1991.
17. M.E. McKnight and J.W. Martin, "Detection and Quantitative Characterization of Blistering and Corrosion of Coatings on Steel Using Infrared Thermography," *Journal of Coatings Technology*, vol. 61, no. 775, 1989, p. 57.
18. M. Pourbaix, "The Electrochemical Basis for Localized Corrosion," *Localized Corrosion*, R.W. Staehle, B.F. Brown, J. Kruger, and A. Agrawal [Eds.], National Association of Corrosion Engineers, Houston, TX, 1971, pp. 12-33.
19. D.B. Anderson, "Statistical Aspects of Crevice Corrosion in Seawater," *Galvanic and Pitting Corrosion—Field and Laboratory Studies*, ASTM STP 576, American Society for Testing and Materials, 1976, p. 231.
20. R.A. Dickie, J.S. Hammond, and J.W. Holubka, "Interfacial Chemistry of the Corrosion of Polybutadiene-Coated Steel," *Industrial and Engineering Chemistry Product Research and Development*, vol. 20, no. 2, 1981, p. 339.
21. H. Leidheiser, W. Wang, and L. Igetoft, "The Mechanism for the Cathodic Delamination of Organic Coatings from a Metal Surface," *Progress in Organic Coatings*, vol. 11, 1983, p. 19.
22. E.L. Koehler, "The Mechanism of Cathodic Disbondment of Protective Organic Coatings—Aqueous Displacement at Elevated pH," *Corrosion*, vol. 40, no. 1, 1984, p. 5.

23. J.F. Watts and J.E. Castle, "The Application of X-Ray Photoelectron Spectroscopy to the Study of Polymer-to-Metal Adhesion," *Journal of Materials Science*, vol. 19, 1984, p. 2259.
24. W. Funke, "The Role of Adhesion in Corrosion Protection by Organic Coatings," *Journal of the Oil Colour Chemists Association*, vol. 68, no. 9, 1985, p. 229.
25. P. Walker, "The Effect of Water Upon Adhesion of Surface Coatings: Part I," *J. Paint Technology*, vol. 31, no. 8, 1967, p. 22.
26. P. Walker, "The Effect of Water Upon Adhesion of Surface Coatings, Part II," *J. Paint Technology*, vol. 31, no. 9, 1967, p. 15.
27. M.T. Goosely, "Chapter 8, Permeability of Coatings and Encapsulants for Electronic and Optoelectronic Devices," *Polymer Permeability*, J. Comyn [Ed.], Chapter 8, 1985, p. 309.
28. H. Leidheiser, Jr. and W. Funke, "Water Disbondment and Wet Adhesion of Organic Coatings on Metals: A Review and Interpretation," *Journal of the Oil Colour Chemists Association*, vol. 70, no. 5, 1987, p. 121.
29. A.L. Glass and J. Smith, "A Radiochemical Investigation of the Effect of Pigment on the Diffusion of Ions Through Protective Films," *Journal of Paint Technology*, vol. 39, no. 511, 1967, p. 490.
30. W. Funke, "Corrosion Tests for Organic Coatings—A Review of Their Usefulness and Limitations," *Journal of the Oil Colour Chemists Association*, vol. 62, 1979, p. 63.
31. R.M. Kain, "Evaluation of Crevice Corrosion," *Metals Handbook, Volume 13*, 9th Edition, American Society of Metals, Metals Park, OH, 1987, p. 303.
32. D.A. Jones, *Principles and Prevention of Corrosion*, MacMillan, New York, 1992.
33. M. Stratmann, A. Leng, W. Fürbeth, H. Streckel, H. Gehmecker, and K.H. Grosse-Brinkhous, "The Scanning Kelvinprobe—A New Technique for the In Situ Analysis of the Delamination of Organic Coatings," *Proceedings of the 20th International Conference in Organic Coatings Science and Technology*, Athens, Greece, July 4-8, 1994.
34. H.H. Uhlig, *Corrosion and Corrosion Control*, Wiley, New York, 1971, pp. 92-126.

35. M. Cohen, "Dissolution of Iron," *Corrosion Chemistry*, G.R. Brubaker and P.B.P. Phipps, [Eds.], ACS Symposium Series 89, American Chemical Society, Washington, D.C., 1979, pp. 126-152.
36. E. McCafferty, "Use of Activity Coefficients to Calculate Conditions Within a Localized Corrosion Cell on Iron," *Journal of the Electrochemical Society: Science and Technology*, vol. 128, 1981, p. 40.
37. W.W. Kittelberger and A.C. Elm, "Water Immersion Testing of Metal Protected Paint-Role of Electro-Osmosis in Water Absorption and Blistering," *Industrial Engineering Chemistry*, vol. 39, 1947, p. 876.
38. W. Funke, "Blistering of Paint Films and Filiform Corrosion," *Progress in Organic Coatings*, vol. 9, 1981, p. 29.
39. G.E. Zaikov, A.P. Iordanskii, and V.S. Markin, *Diffusion of Electrolytes in Polymers*, VSP, Utrecht, The Netherlands, 1988.
40. J.J. Ritter and M.J. Rodriguez, "Corrosion Phenomena for Iron Covered with a Cellulose Nitrate Coating," *Corrosion*, vol. 38, no. 4, 1982, p. 223.
41. T. Nguyen and C. Lin, "In Situ Measurement of Chloride Ion at the Coating/Metal Interface," *Journal of Adhesion*, vol. 33, 1991, p. 241.
42. E.L. Koehler, "The Influence of Contaminants on the Failure of Protective Organic Coatings on Steel," *Corrosion*, vol. 33, no. 6, 1977, p. 209.
43. J.J. Ritter and J. Kruger, *Corrosion Control by Organic Coatings*, H. Leidheiser, Jr., [Ed.], National Association of Corrosion Engineers, Houston, TX, 1981, p. 28.
44. J.W. Martin, M.E. McKnight, T. Nguyen, and E. Embree, "Continuous Wet vs. Cyclic Wet-Dry Salt Immersion Results for Scribed Coated Steel Panels," *Journal of Coatings Technology*, vol. 61, no. 772, 1989, p. 39.